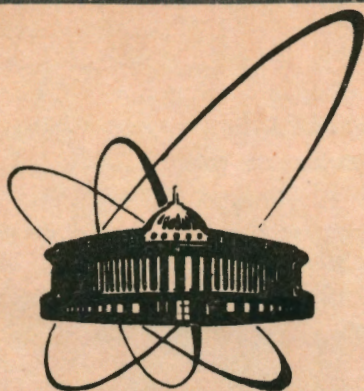


92-372



ОБЪЕДИНЕННЫЙ  
ИНСТИТУТ  
ЯДЕРНЫХ  
ИССЛЕДОВАНИЙ  
ДУБНА

E1-92-372

A.V.Bannikov, G.A.Chelkov, Z.V.Krumstein,  
V.I.Petrukhin, L.S.Vertogradov, J.Bohm<sup>1</sup>, K.Piska<sup>1</sup>,  
A.K.Javrishvili<sup>2</sup>, T.A.Lomtadze<sup>2</sup>, E.G.Tskhadadze<sup>2</sup>

MEASUREMENT AND PROCESSING OF GAMMAS  
ACCOMPANYING MUON PAIRS IN THE  
REACTION  $\pi^- C \rightarrow \mu^+ \mu^- + \gamma + X$  AT 38 GeV

Submitted to «Nuclear Instruments and Methods»

---

<sup>1</sup>Institute of Physics CSASc, Prague, Czechoslovakia

<sup>2</sup>Institute of Physics of GAS, Tbilisi, Georgia

## 1 Introduction

A possibility of detecting gamma quanta in a streamer chamber of the magnetic spectrometer RISK and determining their parameters was rather important for this experiment (SERP-E-151).

First, the contribution of the radiative decay  $\chi_c \rightarrow \gamma J/\psi$  to production of  $J/\psi$ -mesons was estimated [1]. Secondly, the possibility of directly observing Dalitz decays of resonances  $\eta \rightarrow \mu^+ \mu^- \gamma$ ,  $\eta' \rightarrow \mu^+ \mu^- \gamma$  and  $\omega \rightarrow \mu^+ \mu^- \pi^0$  in the region of small masses  $M_{\mu\mu} \leq M_\rho$  (on the basis of the world's best statistics) allowed us to calculate its share in the spectrum of  $\mu^+ \mu^-$ -pairs [2]. These resonances were found to be a dominating source of muon pairs in the region of  $M_{\mu\mu} < 0.6 \text{ GeV}/c$ . This fact essentially changed the idea about the probability of production of "anomalous" dileptons, which was predicted in previous experiments to be about  $(35 \pm 13)\%$  at  $x_F > 0.4$ . Thirdly, registration of  $\gamma$  quanta allows one to study decays of other resonances, e.g.  $a^0(980) \rightarrow \eta \pi^0$ , to determine their role in formation of the dimuon spectrum and to find the accompanying particles, e.g.  $\omega \rightarrow \pi^+ \pi^- \pi^0$  [3].

Unlike previous streamer chamber experiments [4-6], where converters based on materials of large atomic weight were only used to identify electrons and positrons and to count the number of  $\gamma$  quanta, our experiment was the first to involve measurement of momentum and angular characteristics of photons. This made us solve some methodical problems connected with corrections for radiation losses of electrons in converters, selection of  $\gamma$  quanta, rejection of shower photons, etc, which will be the subject of this paper.

The experimental material contains  $\sim 7300 \mu^+ \mu^-$  pair production events, where  $\sim 6260 \gamma$  conversions were registered. About 3370 events with a non-zero number of photon conversions were taken for analysis.

## 2 Targets and converters in streamer chamber

The main part of the spectrometer RISK was a three-gap streamer chamber of working volume  $(4.7 \times 0.9 \times 0.8) \text{ m}^3$ , placed in a magnetic field of 1.5 T [7, 8]. A bipolar high-voltage system [9] supplied power to the chamber with electric field pulses up to 20 kV/cm, their duration being

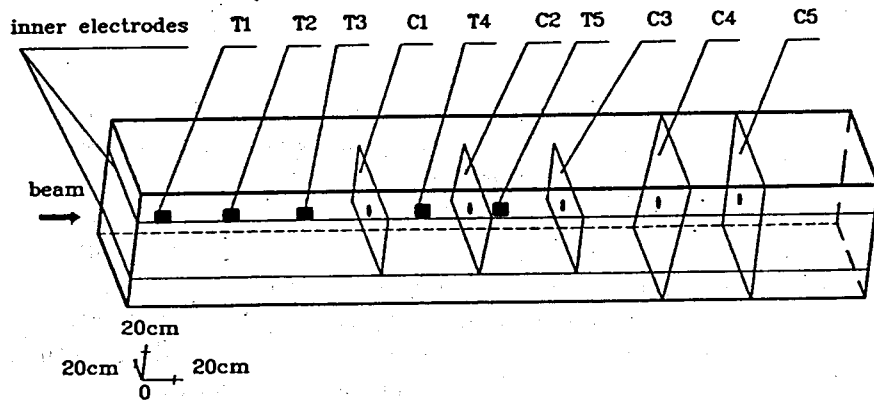


Figure 1: Location of targets (T) and converters (C) in the sensitive volume of a streamer chamber.

$\sim 18$  ns. The chamber was filled with a working mixture of He ( $\sim 50\%$ ) and Ne ( $\sim 50\%$ ) at the atmospheric pressure. Small additions of an electronegative gas  $\text{SF}_6$  allowed the memory time of the streamer chamber to be reduced to 1-2 ms. Four pairs of lenses viewed the sensitive volume of the chamber. The field of view of each pair covered a section  $\sim 120$  cm long [10, 11].

The number of converters and targets, their position in the streamer chamber depended mainly on the requirements of the experiment on production of  $\mu^+\mu^-$  pairs and  $J/\psi$ -particles. To detect the radiative decay  $\chi_c \rightarrow \gamma J/\psi$ , when the average  $\gamma$  quantum momentum is  $\langle p_\gamma \rangle = 2.8$  GeV/c, the version with five targets and five converters proved to be the most suitable (Fig. 1).

A target consisted of two elliptic carbon segments 4.8 cm by 3.6 cm in size, placed at a distance of 3.8 cm from each other downstream. Each segment was 1.8 cm thick, which corresponded to 2.8% of the pion interaction length and 7.2% of the radiation length. Both segments were placed in a cylinder-shaped plexiglas shell 8 cm in diameter, both its ends closed with lavsan film covers 50-70  $\mu\text{m}$  thick. The distance between the covers was 8 cm. Freon was used as an insulating gas forced through the shell.

The five converters (C1-C5) were assembled from plates  $43 \times 18$  cm<sup>2</sup>

and  $43 \times 38$  cm<sup>2</sup> in size and averagely 0.47 cm thick, made of lead glass TF5 [12]. The converters covered the cross section of the chamber either in the middle gap (3 converters – C1-C3) or in all three gaps (2 converters – C4, C5). The converters C2 and C4, placed at the boundary of the field of view of the lenses, are tilted at about 6° to reduce their “shadow” to a minimum and allow observation of electron tracks from the point where they leave the converter.

The choice of the converter thickness depends on two factors. On the one hand, the  $\gamma$  quantum registration efficiency increases with the converter thickness. On the other hand, bremsstrahlung energy losses and fluctuations also increase, which leads to a larger error in determination of the  $\gamma$  quantum energy. The thickness chosen to correspond to  $\sim 23\%$  of  $X_R$  is a kind of compromise.

The surface of the converters is covered with paper or cloth impregnated with epoxy resin to smooth a little the sharp change in dielectric permittivity on the glass-gas surface (the dielectric constant of lead glass is  $\epsilon \sim 7 - 8$ , the dielectric constant of epoxy resin is  $\epsilon \sim 2.4$ ) and to increase mechanical strength. A layer of black paint is applied to the surface of the converters to avoid flashes and reflections.

Holes 7 cm in diameter are cut in the plates for a primary beam. Since the beam is deflected by the magnet field, the centres of the holes are displaced with respect to chamber symmetry axis. As the electric field is “ousted” by the dielectric, there is a region of its higher intensity in the close vicinity of the converter and hole edges. That is why the edges are separated from the working gas in the chamber.

Typical cases of  $\gamma$  quantum conversion are shown in photographs (Fig. 2).

The acceptance of the installation for detection of  $\gamma$  quanta depends on the position of the target in which the interaction occurred, the kinematic characteristics and the probability of photon conversion. The radiation unit of length of the converter was calculated in accord with the weight part of each component of lead glass –  $R = 9.48$  g/cm<sup>2</sup> (1.99 cm). The absorption coefficient  $\mu(E)$ , which determines the probability of a  $\gamma$  quantum absorbing the energy E over a radiation unit of length, was calculated by the known Bethe-Heitler formulae [13] and approximated by a polynomial. The dependence of the acceptance on the Feynman

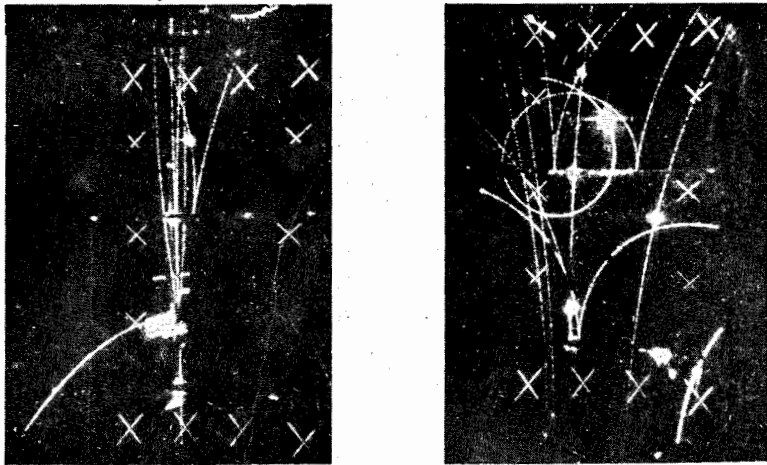


Figure 2: Typical cases of  $\gamma$  quantum conversion (3rd quarter of sensitive volume: target T5, converters C2 and C3).

variable  $x_F$  and the transverse momentum  $p_T$  of  $\gamma$  quanta from the third target is given in Fig. 3. As to the registered photons, their mean weight over all the experimental material is  $\sim 2.6$ .

Two factors determined the length over which tracks were measured: the particle momentum and the distance between the converters. Low-energy particles ( $E < 0.25$  GeV) were measured over the maximum length (lower limit was about 3-4 cm, which corresponded to momentum  $\sim 10$ -20 MeV/c). At higher energies of  $e^+$  and  $e^-$  the track section to be measured was limited by the distance between converters equal to  $\sim 60$  cm, which allowed the accuracy  $dp/p \sim 0.04 * p$  [GeV/c]. The coordinates of the  $\gamma$  quantum conversion point  $V_\gamma$  were found in compliance with the condition that the sum of squares of distances of the vertex from the closest points on the particle trajectories was a minimum. The accuracy of the vertex reconstruction is illustrated by the mean difference between  $V_\gamma$  and the intersection point  $V_c$  of the  $\gamma$  quantum momentum vector and the centre of the converter:  $\langle V_\gamma - V_c \rangle = -0.84 \pm 0.12$  mm.

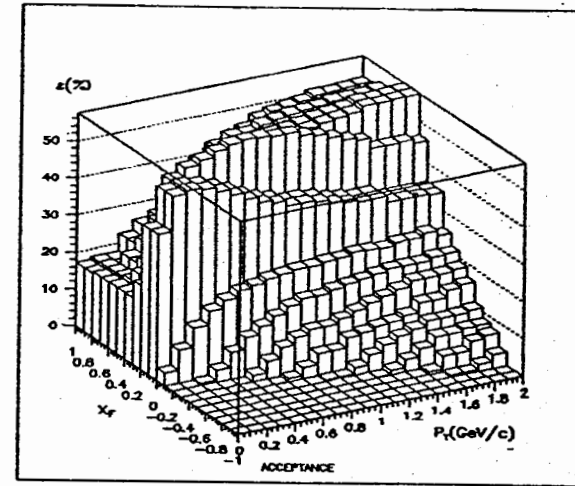


Figure 3: Acceptance as a function of the transverse momentum  $p_T$  and the Feynman variable  $x_F$  for  $\gamma$  quanta from the third target.

### 3 Analysis of gamma accompaniment of muon pairs

Interaction of photons with the converter material resulted in production of single electrons  $e^-$  (9.6%), electron-positron pairs  $e^+e^-$  (86.1%), triplets  $e^+e^-e^-$  (2.5%) and quartets  $e^+e^+e^-e^-$  (1.8%). Only  $e^+e^-$  pairs were taken for analysis because most single electrons were rejected by momentum cut-off, and triplets and quartets, though producing little effect on statistics, caused larger (as compared with  $e^+e^-$ ) errors in determination of  $\gamma$  quantum parameters.

To reject interaction of non-charged particles with a converter and decays of  $K^0$ - and  $\Lambda$ -particles near the converter, a constraint  $M_{e^+e^-}^2 \leq 0.01$  (GeV/c<sup>2</sup>)<sup>2</sup> was imposed on the effective  $e^+e^-$  pair mass, which led to a loss of 2.6% of events. The angle between the electron and the positron can help to determine the photon energy more precisely in some cases, because it bears a relation to the part of the momentum transferred to the nucleus in whose field a pair is produced [14]. In this case, however, the experimental values of the angle considerably differed from the theoretical ones owing to rescattering of electrons in the converter material

and inaccuracy in measurement of their escape angles. That is why the quantity  $M_{e^+e^-}$  was not used after that, it was taken to be zero and the energy was taken to be equal to the momentum.

The fact that there were five relatively thick targets in the beam can be the reason both for simultaneous escape of photons from different targets and for their production in a secondary interaction in the same target. It is important to estimate the number of "alien"  $\gamma$  quanta and to get rid of them if possible. For this purpose one can employ the  $\gamma$  quantum parallax PARX, i.e. the angle between the  $\gamma$  quantum momentum vector and the vector connecting the primary interaction vertex with the reconstructed vertex of the  $e^+e^-$  pair (Fig. 4). This quantity was assumed to originate from a "natural" source: errors in measurement of momenta and escape angles of electrons, their energy losses in a converter. It is confirmed by similarity of the dependence of the mean value  $\langle \text{PARX} \rangle$  on the mean photon momentum and the distribution of errors in the azimuthal and polar angles  $\langle d\lambda_\gamma \rangle$  and  $\langle d\varphi_\gamma \rangle$ . As the momentum increases to  $\sim 0.7$  GeV/c, the value  $\langle \text{PARX} \rangle$  falls down from  $\sim 120$  mrad to  $\sim 35-40$  mrad and then changes but slightly;  $\langle d\lambda_\gamma \rangle$  and  $\langle d\varphi_\gamma \rangle$  behave in the same manner but in other angle ranges. For checking the parallax was simulated in the following way. The photon momentum vector was rotated such that  $\text{PARX} = 0$ . Then radiation losses of each electron from the  $e^+e^-$  pair were simulated uniformly within the average losses calculated for this purpose. After calculation of new  $\gamma$  quantum parameters corrections for measurement errors  $\langle d\lambda_\gamma \rangle$  and  $\langle d\varphi_\gamma \rangle$  were introduced on the assumption that they obey the Gaussian distribution. The only free parameter, error distribution dispersion, was chosen by comparing with the experimental histogram. The result of this comparison (normalized to the distribution maximum) is shown in Fig. 4. The curve is satisfactory for the initial part of experimental PARX value, but not for the "tail" of the distribution, which extends to angles of  $\sim 500$  mrad. It follows from this comparison that from angles of  $\sim 150$  mrad (Fig. 4b) a considerable number of  $\gamma$  quanta can be considered to be "alien". This cut-off leads to a loss of 5% of photons, most of which, however, are of low energy.

The effective mass spectrum of two gamma quanta, the  $\pi^0$ -meson peak shape, its position and width were a kind of indicator for correct-

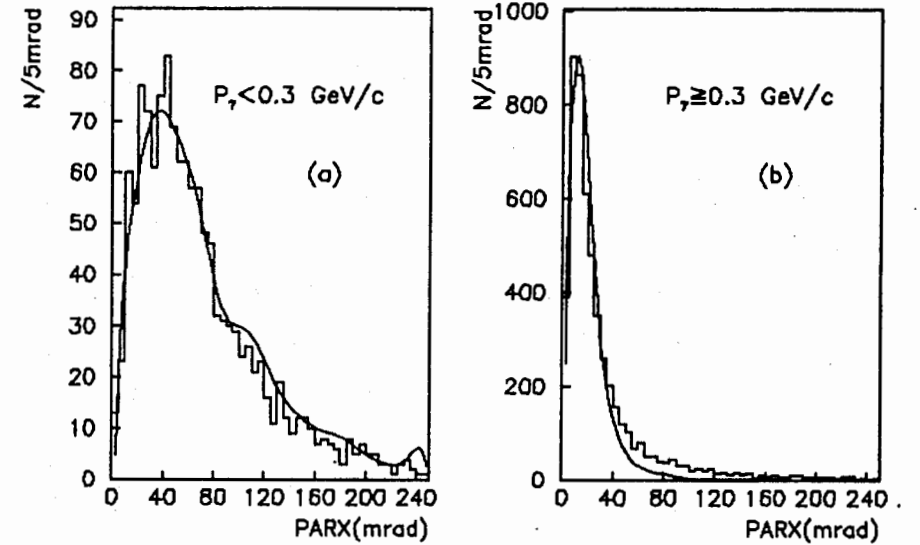
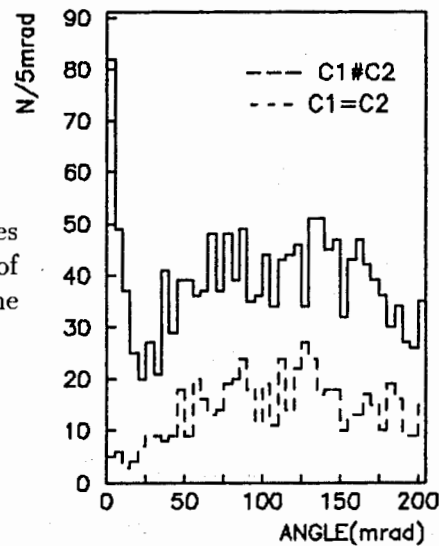


Figure 4: Distribution in the parallax of photons with momentum  $p_\gamma < 0.3$  GeV/c (a) and  $p_\gamma \geq 0.3$  GeV/c (b). The histogram is the experiment, the curve is the simulation.

ness of operations with photons. For example, rotation of the  $\gamma$  quantum momentum vector by angle PARX resulted in a considerably narrower  $\pi^0$  signal and a sharp peak in the region  $M_{\gamma\gamma} < 20$  MeV/c<sup>2</sup>, which is not seen in the initial spectrum. As already mentioned, in 1.8% of events there were  $e^+e^+e^-e^-$  combinations resulted from conversion of a bremsstrahlung photon emitted by an electron from the  $e^+e^-$  pair produced by an initial  $\gamma$  quantum [15]. It would be strange not to observe the same effect but at different converters. It is seen from the distribution of angles among momentum vectors of  $\gamma$  quantum pairs detected in the same and in different converters (Fig. 5) that secondary photons are in the range of angles from 0 to 20 mrad with respect to the primary one, and the number of those placed in this category by chance (it can be estimated by the bottom histogram) is not more than 1.6% of the total number of combinations. Of the two photons selected in this way we excluded from consideration the last one, if it took away a fraction of energy, or both, if their momenta were close in value.

The converters were not thick enough for development of a multipar-

Figure 5: Distribution of angles between the momentum vectors of pairs of  $\gamma$  quanta registered in the same and in different converters.



ticle shower; yet, they were thick enough for bremsstrahlung losses of electrons to be noticeable. To calculate them, we found the most probable  $\gamma$  quantum conversion point, which was at such a place that with the given converter thickness there were equal total probabilities for a photon of known momentum and escape angles to produce an  $e^+e^-$  pair before and after this point. Then the range of each electron before leaving the converter was determined in accordance with its angles. It is on this range that the energy losses were calculated in relation to the electron momentum. The allowance for the losses resulted, among other things, in a slight ( $\leq 10$  MeV/c<sup>2</sup>) displacement of the  $\pi^0$  peak.

Finally, to reduce the background and exclude photons that do not practically contribute to the  $\pi^0$  signal, we determined the lower limit of the  $\gamma$  momentum spectrum. For this purpose  $\gamma\gamma$  spectra were constructed on condition that the momentum of one or both photons is below a certain value, which was changed with a step of 50 MeV/c. The  $\pi^0$ -meson peak was found to appear when a  $\gamma$  momentum exceeds 150 MeV/c and/or the sum of the momenta exceeds 400 MeV/c. Photons that failed to meet this requirement were rejected.

#### 4 Conclusion

The methodical problems of placing a set of lead glass gamma converters in a three-gap streamer chamber 80 cm deep are solved. Unlike the case in other streamer chamber experiments, where converters were used only for identification of electrons and photons, in this experiment the angular and momentum characteristics of  $\gamma$  quanta were measured for the first time.

While processing the gamma quantum measurements, we have done the following operations:

- only electron-positron pairs from converters were selected for analysis (86.1%);
- pairs with a more than 50% relative error,  $dp_e/p_e$ , in measurement of the momentum of one of the electrons were rejected (0.9% of electrons);
- pairs with the effective mass  $M_{e^+e^-}^2 \leq 0.01$  (GeV/c<sup>2</sup>)<sup>2</sup> were rejected (2.6%);
- photons with the parallax PARX larger than 150 mrad were rejected (4.8%);
- correction for the parallax were made;
- corrections for radiation losses of electrons were made;
- shower photons were excluded (6.1%);
- in separation of  $\pi^0$ -mesons the lower limit of the  $\gamma$  momentum spectrum was 150 MeV/c and/or the sum of the momenta of two  $\gamma$  quanta was 400 MeV/c.

It should be mentioned that the percentage of losses in each of the above paragraphs is given irrespective of the others. Since a  $\gamma$  quantum is often rejected on the basis of several criteria at a time, the total losses are a small part of the data obtained. For example, most of the photons rejected for the parallax were in the range of small momenta and can be excluded from the analysis by the last paragraph.

The final effective mass spectrum of two  $\gamma$  quanta is given in Fig. 6a. The distribution was fitted by the sum of two functions, the polynomial and the Gaussian. The following parameters were obtained:  $M_{\pi^0} = (135.5 \pm 1.1)$  MeV/c<sup>2</sup>,  $\sigma_{\pi^0} = (9.4 \pm 1.1)$  MeV/c<sup>2</sup>. To simulate production of  $\pi^0$ -mesons with allowance of the installation acceptance, the momentum spectra of  $\pi^+(\pi^-)$ -mesons were used as initial particles, or pa-

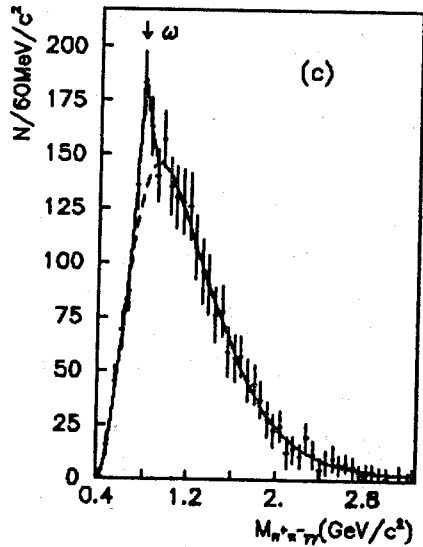
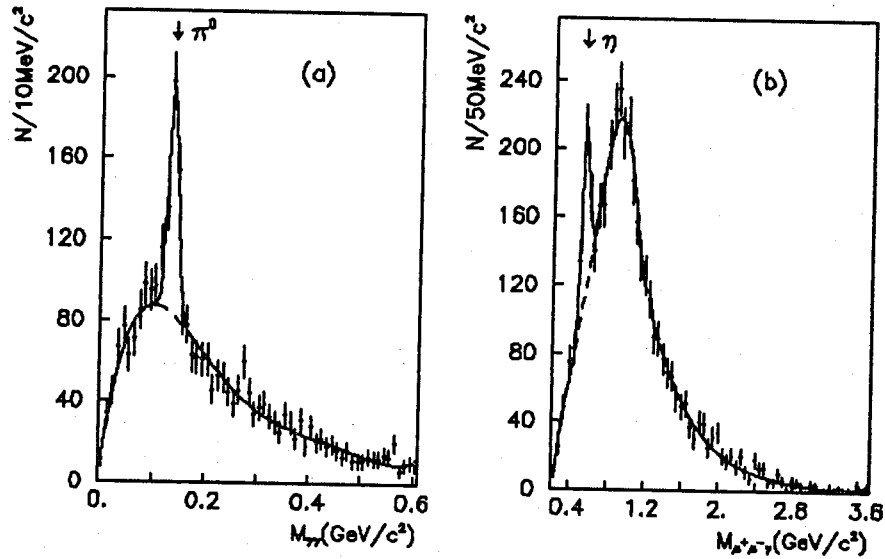


Figure 6: Effective mass spectrum of  $\gamma\gamma$  (a),  $\mu^+\mu^-\gamma$  (b) and  $\pi^+\pi^-\gamma\gamma$  (c). The curves are the results of fitting.

rameters of the particle were simulated within the appropriate kinematic limits. Allowance for corrections discussed above led to a  $\gamma\gamma$  spectrum shape close to the experimental one. Another result is connected with  $\eta$ -mesons decaying into two photons. Simulation showed that, first, their number that can be registered by the installation is 60% of the number of  $\pi^0$ -mesons; secondly, the error "smearing" results in a wide peak ( $\sigma_\eta \sim 40 \text{ MeV}/c^2$ ). If the production cross section and the probability of the decay into two  $\gamma$  quanta is taken into account, there must be a very weak manifestation of the  $\eta$ -meson signal.

To check the above operations in another way the effective mass spectra of  $\mu^+\mu^-\gamma$  and  $\pi^+\pi^-\gamma\gamma$  were constructed (Fig. 6b and 6c). In the  $\mu^+\mu^-\gamma$  distribution the  $\gamma$  quantum momenta was cut off by the lower limit of 300 MeV/c. In the latter case there was an additional constraint imposed on the effective mass of a photon pair:  $100 < M_{\gamma\gamma} < 170 \text{ MeV}/c^2$ , only one combination closest to the  $\pi^0$  mass was selected in an event. The distribution was fitted similarly to  $\pi^0$ . The parameters obtained are  $M_\eta = (549.5 \pm 5.4) \text{ MeV}/c^2$ ,  $\sigma_\eta = (26.6 \pm 4.8) \text{ MeV}/c^2$ ;  $M_\omega = (782.5 \pm 10.9) \text{ MeV}/c^2$ ,  $\sigma_\omega = (33.3 \pm 11.8) \text{ MeV}/c^2$ . The values of these parameters prove the procedure of data processing and introduction of corrections to be correct.

The authors express their sincere gratitude to T.I. Kotova and T.P. Saenko for assistance in preparing the paper.

## References

- [1] J.Jani et al., Preprint JINR E1-87-397, Dubna, 1987.
- [2] A.V.Bannikov et al., Preprint JINR E1-89-486, Dubna, 1989.
- [3] RISK Collab., J.Böhm, Pittsburgh Workshop on Soft photon and lepton pair production (September 1990).
- [4] K.Eggert et al., Nucl. Instr. and Meth. 126 (1975) 477.
- [5] M.I.Dayon et al., Nucl. Instr. and Meth. 116 (1974) 329.

- [6] K.Bunnel et al., Proc. of the 1th Int. Conf. on Streamer Chamber Technology, AN1-8055, Argonne, 1972.
- [7] A.K.Javrishvili et al., Nucl. Instr. and Meth. 177 (1980) 381.
- [8] L.S.Vertogradov et al., Preprint JINR P13-8078, Dubna, 1980, in Russian.
- [9] L.S.Vertogradov et al., Prib. Tekh. Exp. 3 (1978) 31, in Russian; A.V.Bannikov et al., Prib. Tekh. Exp. 2 (1985) 36, in Russian.
- [10] E.M.Andreev et al., Preprint JINR 13-8550, Dubna, 1975, in Russian.
- [11] E.G.Boos et al., Z.Phys.C - Particles and Fields 26 (1984) 43; H.Bärwolff et al., Z.Phys.C - Particles and Fields 31 (1986) 64.
- [12] A.V.Bannikov et al., Prib. Tekh. Exp. 2 (1989) 69, in Russian.
- [13] B.Rossi, K.Greisen, Rev. Mod. Phys. 13 (1941) 240; B.Rossi, High Energy Particles, Englewood Cliffs, N.J.,1952.
- [14] I.P. Ivanenko, Electromagnetic Cascade Processes, Moscow University, 1972, in Russian.
- [15] S. Hayakava, Cosmic Ray Physics, N.J.,1969.

Received by Publishing Department  
on September 1, 1992.

Банников А.В. и др.

E1-92-372

Измерение и обработка гамма-сопровождения  
мюонных пар в реакции  $\pi^+C \rightarrow \mu^+\mu^- + \gamma + X$  при 38 ГэВ

В чувствительном объеме стримерной камеры магнитного спектрометра РИСК при проведении эксперимента SERP-E-151 по изучению эксклюзивных процессов рождения мюонных пар и  $J/\psi$ -частиц в  $\pi^+C$ -взаимодействиях при 38 ГэВ размещался набор углеродных мишеней и конверторов, изготовленных из свинцового стекла. Представлены их конструкция и характеристики. Осуществлено измерение импульсных и угловых спектров  $\gamma$ -квантов. Приводится описание процесса обработки полученного материала, включающего в себя отбор фотонов, введение поправок на их параметры и элементы моделирования. Для иллюстрации показаны спектры эффективных масс  $\gamma\gamma$ ,  $\mu^+\mu^-\gamma$  и  $\pi^+\pi^-\gamma\gamma$ .

Работа выполнена в Лаборатории ядерных проблем ОИЯИ.

Препринт Объединенного института ядерных исследований. Дубна 1992

Bannikov A.V. et al.

E1-92-372

Measurement and Processing of Gammas Accompanying  
Muon Pairs in the Reaction  $\pi^+C \rightarrow \mu^+\mu^- + \gamma + X$  at 38 GeV

A set of carbon targets and lead glass converters were placed in the sensitive volume of a streamer chamber of the magnetic spectrometer RISK in the experiment SERP-E-151 on the study of exclusive processes of production of muon pairs and  $J/\psi$ -particles in  $\pi^+C$  interactions at 38 GeV. The design and characteristics of the targets and converters are given. Momentum and angular spectra of  $\gamma$  quanta are measured. The processing of the data obtained is described, including selection of photons, correction for their parameters and elements of simulation. Effective mass spectra of  $\gamma\gamma$ ,  $\mu^+\mu^-\gamma$  and  $\pi^+\pi^-\gamma\gamma$  are shown for illustration.

The investigation has been performed at the Laboratory of Nuclear Problems, JINR.

Preprint of the Joint Institute for Nuclear Research. Dubna 1992